

Atomic scale imaging of albite feldspar, calcium carbonate,
rectorite, and bentonite using atomic force microscopy

Barney Drake

Imaging Services, SPM Laboratory Service
5370 Hollister Ave, Suite K, Santa Barbara, CA 93111

Roland Hellmann

Universite Joseph Fourier, L.G.I.T-I.R.I.G.M, B.P. 53X
38041 Grenoble Cedex, France

C. Steven Sikes

University of S. Alabama, Mineralization Center
Department of Biological Sciences, Mobile, AL 36688

Mario L. Ocelli

Georgia Tech Research Institute
Georgia Institute of Technology, Atlanta, GA 30332

ABSTRACT

Atomic force microscopy (AFM) was used to investigate the (010) surface of Amelia albite, the basal and (001) planes of CaCO₃ (calcite), and the basal planes of rectorite and bentonite. Atomic scale images of the albite surface show six sided, interconnected en-echelon rings. Fourier transforms of the surface scans reveal two primary nearest neighbor distances of 4.7 and $4.9 \pm 0.5 \text{ \AA}$. Analysis of the images using a 5 Å thick projection of the bulk structure was performed. Close agreement between the projection and the images suggests the surface is very close to an ideal termination of the bulk structure. Images of the calcite basal plane show a hexagonal array of Ca atoms measured to within $\pm 0.3 \text{ \AA}$ of the 4.99 Å predicted by x-ray diffraction data. Putative images of the (001) plane of carbonate ions, with hexagonal 5 Å spacing, are also presented and discussed. Basal plane images of rectorite show hexagonal symmetry with $9.1 \pm 2.5 \text{ \AA}$ spacing, while bentonite results reveal a $4.9 \pm 0.5 \text{ \AA}$ nearest neighbor spacing.

1. INTRODUCTION

Since the invention of the AFM in 1986 by Binnig, Quate, and Gerber¹, the AFM has produced atomic scale images of a variety of materials. Published atomic scale results include images of metal thin films², minerals³, and ionic crystals⁴. We report here atomic scale images of Amelia albite, calcium carbonate (calcite), rectorite, and bentonite (montmorillonite). In this paper the AFM results will be presented and discussed in brief leaving more detailed analysis to other publications⁵.

1.a. Albite

Amelia albite was chosen for study because of its general geologic significance and its bulk structure is well known. The goal of this study was to determine if the natural cleavage (010) surface is an ideal termination of the bulk structure. From a preliminary comparison of nearest neighbor distances measured from the AFM images with those from a 5 Å thick surface projection based on x-ray and neutron diffraction data⁶, close agreement suggests the surface is close to an ideal termination of the bulk. The largest difference in nearest neighbor distances was 0.2-0.4 Å.

1.b. Calcite

The importance of the bio-mineral calcite, is readily apparent as it is the most abundant bio-mineral found in nature. Recent work by Friedbacher⁷ et.al. and Hilner⁸ et.al. underscored the importance of calcite. The purpose of our study of the calcite atomic scale landscape is to better understand the mechanisms and interactions of proteins and peptides that regulate the formation of calcite bio-minerals.

1.c. Rectorite and bentonite

Rectorite is an interstratified layered silicate mineral consisting of a regular stacking of mica-like and montmorillonite-like layers⁹. Bentonite is the name of a rock containing more than 90% montmorillonite, a clay mineral consisting of two layers of silicon in a tetrahedral coordination holding a layer of aluminum atoms in octahedral coordination. The study of rectorite and bentonite is important because these clays could be used as catalysts in petrochemical processes since by ion exchanging their charge compensating cations (Na or Ca) with bulky oxyocations of Al or Zr, it is possible to generate microporous structures with the thermal stability required in fluid catalytic cracking and fixed bed applications such as hydrocracking^{10,11,12}. The properties of these clay catalysts have been reviewed elsewhere¹³.

2. EXPERIMENTAL

All samples were imaged with a NanoScope II¹⁴ contact mode AFM (Digital Instruments). The optical lever design^{15,16} used in the AFM has been described in detail in previous publications³. 120 μ m Si₃N₄ cantilevers ($k \approx 0.6$ N/m) with integral tips¹⁴ were used on all samples. Forces while imaging ranged from 1 to 100 nN. The albite, rectorite, and bentonite images were produced with a 1 μ m x 1 μ m (max.) piezo-scanner. The calcite results were obtained using a 12 μ m x 12 μ m (max) scanner. The scanners were calibrated with both mica and graphite (HOPG) to within \pm 5-10%. All atomic scale images were processed by subtracting out a plane, then filtered using a two dimensional fast Fourier transform. All peaks were kept with the high frequency noise removed.

2.a. Albite

The albite from Amelia Court House, Virginia was supplied by Wards Scientific Establishment. The specimen was compositionally pure as determined by microprobe analysis¹⁷. The AFM images were taken from a single cleavage fragment that was imaged four times with four different cantilevers over a 3 month period. With each cantilever atomic resolution was achieved within one hour and lasted for at least one half hour.

2.b. Calcite

The calcite samples were single crystals grown onto a glass coverslip. The coverslip was placed into a round bottom flask where crystallization spontaneously occurred after six minutes in 60 ml of 10mM Ca²⁺, 8mM inorganic carbon, at 20°C with initial Ph 8.3¹⁸. The crystals varied in size from approximately 2 μ m x 2 μ m (roughly rhombohedral) to 7 μ m x 7 μ m. The crystals grew preferentially with the c-axis perpendicular to the flat glass surface. The atomic resolution images presented here were all from the top surface, along the c-axis. Calcite crystals are arranged as alternating planes of calcium atoms and carbonate ions along the c-axis^{19,20}. The convention is to call the calcium plane the basal plane and the carbonate plane the (001) plane.

2.c. Rectorite

A rectorite sample from Garland County, Arkansas was obtained from the Clay Mineral Society Repository. The samples consisted of quartz aggregates containing 10-20% clay from which the rectorite flakes were obtained using a procedure described elsewhere¹². After beneficiation the sample contained 49.5% SiO₂, 34.4% Al₂O₃; after drying in air at 100°C gave an x-ray pattern in excellent agreement with JCPDS pattern No. 25-781 for rectorite¹². Trace amounts of kaolin and quartz were present in the sample. Rectorite flakes were then submitted to AFM without further treatment.

2.d. Bentonite

The bentonite sample studied here was obtained from the Southern Clay Products of Gonzales, Texas. The sample contained about 71% SiO₂, 15.7% Al₂O₃, 3.6% MgO, and 1.7% CaO and has a cation exchange capacity of 80 meq/100g. X-ray diffraction and ²⁹Si-NMR data (not shown) have indicated that the sample contains minor amounts of silica impurities. The bentonite powder was pressed at 10,000lbs/1min into wafers 2.5cm in diameter that were then submitted for AFM analysis.

3. RESULTS AND DISCUSSION

3.a. Albite

From Fig. 1a it is possible to distinguish individual, interconnected, six sided rings. The ring structure, however, is distorted giving center to center spacing varying from ≈ 4.0 to ≈ 5.0 Å. Examining the central ring in Fig. 1a yields 1.8 to 2.0 Å spacing for the shortest internode distance. The larger internode distance ranges from 3.0 to 3.6 ± 0.3 Å. The degree of interconnectedness is also quite variable. Some of the rings show a significant connection while most show a faint to non-existent bridge. Fig. 1c is a low magnification image of the (010) surface. Fig 1a was taken on the square feature in the center of the image.

Our analysis of the AFM images was aided by a comparison of a 5Å thick slice (along the b axis) of a projection of the albite structure. The projection (EMS software) based on an x-ray and neutron diffraction structure refinement of the albite structure.⁵ For the sake of clarity we have used the following non-standard ionic radii: Si⁴⁺=0.20, Al³⁺=0.20, O²⁻=0.50, Na¹⁺=0.70, (all in Å). From the large number of oxygen atoms (32 per unit cell), and their relative size it is clear that the oxygens determine the structural outline of the rings (fig 1d).

In Fig. 1b, the 2.0 × 2.0 nm image shows the sinuous pattern which closely matches the projection. The orientation of the projection was determined by comparing the Fourier transforms of the projection with that of the images. From two dimensional fast Fourier transforms of three different images, two average nearest neighbor distances were measured: 4.7 and 4.9 ± 0.5 Å. The two dominant nearest neighbor distances of the projection were 4.4 and 4.7 ± 0.2 Å. From a ≈ 14 unit cell superposition of the projection onto a 30 × 30 Å AFM image (not shown) there is a good correlation, but the inter-ring spacing in the a and c directions was not quite perfect. There was also a lack of one-to-one correspondence between atoms or atom clusters and the AFM image.

It should be noted that the methods used here are simplistic in this very complex process of surface structure determination. Errors in the analysis could come from the orientation in the superposition of the projection onto the image. The choice of the location and thickness of the slice affects the orientation and inter-planer distances in the projection. Instrument error caused by thermal drift, piezo creep and cantilever buckling could also be a factor in the superposition mis-match. In addition, Auger surface spectroscopy data (unpublished data) on the same type of sample shows the presence of adventitious atmospheric contaminants (nitrogen, carbon, etc.). Thus, the simple act of cleaving a sample in air results in the large-scale adsorption of atoms and molecules on the surface. This process may also play a role in the interpretation of the results.

3.b. Calcite

The AFM image of the basal plane of calcite (fig. 2a) showed a hexagonal structure with a spacing of 5.0 ± 0.3 Å which matches the 4.99 Å spacing measured by x-ray crystallographic data. These results are consistent with previously published AFM images of calcite powder⁷. The atoms of this plane were identified as calcium atoms because of their appearance as single atoms of approximately 1 Å in diameter.

Alternatively, the plane of atoms along the c-axis of calcite could be composed of carbonate ions. Theoretically, the carbonate ion would appear as a carbon atom with 3 coplanar oxygens attached symmetrically. The carbonate ion would comprise a cluster of 2 to 3 Å diameter, each arranged hexagonally at 5 Å spacing with respect to the others.

The calcite crystals were grown with the c-axis exposed, as reported by Addadi and coworkers^{21,22,23}, which potentially provides access to the basal and (001) planes. Our work to date routinely and clearly has revealed basal planes of calcium atoms.

Occasionally, we also have obtained striking images (fig. 2b,c) of planes suggestive of carbonate ions, although the apparent number of atoms per cluster and the atomic spacing have not always matched well with theory. There is the possibility of multiple tip effects in these images.

The presence of calcium versus carbonate planes is interesting crystallographically. It is possible that an exposed calcium plane would be favored energetically versus a carbonate plane. There is also the possibility that the carbonate plane is normally not exposed during crystal growth, which would have implications for the mechanisms of calcite lattice formation.

The availability of surficial calcium or carbonate planes for binding proteins during biological calcite formation may also be significant. Various studies have shown that polyanionic proteins, polyamino acids, and peptides, but not their polycationic counterparts, are powerful inhibitors of calcite and calcium hydroxyapatite formation.^{17,24,25,26,28} On one hand, this might suggest that a polycationic crystal surface, such as the calcium plane of calcite, is available to provide growth sites to which the polyanionic inhibitors bind. On the other hand, it would appear that a polyanionic surface, such as the carbonate plane, is not available.

However, there is evidence that suggests polyanionic biomolecules may be preloaded with soluble calcium, leading to a conformational shift that favors binding to a polyanionic crystal surface, presumably like the carbonate plane^{17,21,22,23}. Thus, it will be useful to determine the identity of the binding sites. These questions lend themselves to evaluation by AFM. Our work in progress is directed to this end.

3.c. Rectorite and bentonite

The SiO₄ units in 2:1 clay minerals, form basal planes containing hexagonal rings of oxygen ions separated by about 5.4 Å; the lateral distance between rings is about 11 Å^{3,29}. The 4.9 ± 0.5 Å nearest neighbor spacing of the bentonite sample shown in fig. 3b is in agreement with this spacing (5.4 Å) obtained from simple geometric considerations and with the spacing (5.1 ± 0.3 Å) found in previous AFM images of montmorillonite³. In all of the montmorillonite images obtained in this study (or reported elsewhere³) the presence of surface cations was not observed.

Images for a sample of Mg-rectorite are shown in fig. 3a. As for montmorillonite, hexagonal arrays of spots are observed. However, the nearest neighbor distance of 9.1 ± 2.0 Å is almost twice as large as the distance observed in montmorillonite. Furthermore, the lateral distance between spots in rectorite is 17 ± 2.0 Å.

Energy dispersive spectroscopy measurements have indicated that the rectorite sample contains 2.1 % MgO, almost twice as much MgO as measured by atomic absorption indicating the existence of a Mg enriched surface³⁰. It is tentatively proposed that the charge compensating Mg-cations are both in the clay expandable (montmorillonite) layers and on the clay platelets surface. A nearest-neighbor distance of 9.1 Å is consistent with the presence of a Mg-ion for every two hexagonal holes. AFM characterization of these montmorillonite and rectorite samples pillared with alumina clusters will be discussed elsewhere³¹.

4. CONCLUSION

4.a. Albite

The images shown here reveal atomic scale details of the albite (010) surface. A projection, based on x-ray and neutron diffraction data was used to analyze the AFM images. A one to one correspondence was found between rings in the projection and the six sided ring structure found in the images, however true atomic resolution was not achieved. Nearest neighbor distances measured on the images were 0.2 to 0.4 Å greater than those taken from the projection. This discrepancy was either caused by instrument error or a lateral relaxation of the surface. Recent work by Hochella³² et. al. shows a slight relation of the (010) albite surface, although the images presented here show that major differences do not exist between the surface and bulk structure.

4.b. Calcite

The atomic resolution images from the basal plane of single crystal calcite show a hexagonal structure with nearest neighbor

spacing of $5.0 \pm 0.3 \text{ \AA}$. This matches the predicted Ca-Ca atom spacing of 4.99 \AA . From these and other results, the properties of calcite such as atomic scale flatness and high reactivity (compared to other common AFM substrates) may lend itself as a substrate for imaging biologic samples.

4.c. Rectorite and bentonite

Fourier transform analysis of the basal plane images of bentonite reveal a $4.9 \pm 0.5 \text{ \AA}$ nearest neighbor spacing while Mg-rectorite images show $9.1 \pm 2.0 \text{ \AA}$ spacing. These preliminary results suggest the Mg-ions on the surface of the rectorite were imaged directly.

5. ACKNOWLEDGEMENTS

The authors would like to thank P.K.Hansma and M. Wilson for preliminary work on the bentonite, H.G.Hansma, G. Kelderman, S. Manne, J. Massie, V. Elings, E.A. Wendt, and C. Smith for useful discussions and assistance. This was supported in part by N.S.F. grant DMB 891460.

6. REFERENCES

1. Binnig, G., Quate, C.F., and Gerber, Ch., "Atomic Force Microscope," *Phys. Rev. Lett.*, 12, 930-933, 1986.
2. Manne, S., et.al., "Imaging metal atoms in air and water using the atomic force microscope," *Appl. Phys. Lett.*, 18, 1758-1759, 1990.
3. Hartman, H., et.al., "Molecular-scale imaging of clay mineral surfaces with the atomic force microscope," 38, 337-342, 1990.
4. Meyer, G. and Amer, N.M., "Optical beam-deflection atomic force microscopy: The NaCl (001) surface," *Appl. Phys. Lett.*, 56, 2100-2101, 1990.
5. Albite: Drake, B. and Hellmann, R., "Atomic force microscopy imaging of the albite (010) surface," *Amer. Mineral.*, 76, 1773-1776, 1991., Bentonite: Occelli, M. L. and Drake, B., submitted to *Journal of Catalysis.*, Calcite: Sikes, C. S., Drake, B., Donachy, J., manuscript submitted.
6. Harlow, G.E. and Brown, G.E., Jr., "Low albite: an x-ray and neutron diffraction study," *Amer. Mineral.*, 65, 986-995, 1980.
7. Friedbacher, G., et. al., "Imaging powders with the atomic force microscope", *Science*, 253, 1261-1263, 1991.
8. Hilner, P.E., et. al., "Atomic scale imaging of calcite growth and dissolution in real time," submitted to *Geology*, 1991.
9. Kodama, H., *Amer. Mineral.*, 51, 1035, 1966.
10. Guan, J., Min, E., and Yu, Z., U.S. Pat. No. 4,757,040 (1986).
11. McCauley, J.R., U.S. Pat. No. 4,952,544 (1990).
12. Occelli, M.L., in "Preparation of catalysts V," Poncelet, G., Jacobs, P.A., Grange, P., Delmon, B., Elsevier, Amsterdam, 287, 1988.
13. Occelli, M.L., in "Keynotes in energy related catalysis," Kaliaguine, S., Ed., Elsevier, Amsterdam, 101, 1991.
14. Digital Instruments, Inc., Santa Barbara, CA 93117.

15. Meyer, G. and Amer, N.M., "Novel optical approach to atomic force microscopy," *Appl. Phys. Lett.*, 53, 1045-1047, 1988.
16. Alexander, S., et.al., "An atomic-resolution atomic force microscope implemented using an optical lever," *J. Appl. Phys.*, 65, 164-167, 1989.
17. Hellmann, R., et.al., "The formation of leached layers on albite surfaces during dissolution under hydrothermal conditions," *Geochimica et Cosmochimica Acta*, 54, 1267-1281, 1990.
18. Wheeler, A.P. and C.S. Sikes, "Matrix-crystal interactions in CaCO₃ biomineralization," *Chemical Perspectives in Biological Mineralization*, 95-131, VCH Publishers, Weinheim, 1989.
19. Bragg, W.H. "X-rays and crystal structure," *Proceedings of the Royal Society of London, A*, 215, 253-274, 1915.
20. Lippmann, F. "Sedimentary Carbonate Minerals," Springer-Verlag, New York. 228, 1973.
21. Addadi, L. and S. Weiner, "Interactions between acidic proteins crystals: stereochemical requirements in biomineralization," *Proceedings of the National Academy of Science USA*, 82, 4110-4114, 1985.
22. Addadi, L., et. al., "A chemical model for the cooperation of sulfates and carboxylates in calcite crystal nucleation: relevance to biomineralization," *Proceedings of the National Academy of Science USA*, 84, 2732-2736, 1987
23. Addadi, L. and S. Weiner, "Stereochemical and structural relations between molecules and crystals in biomineralization," *Biomineralization: Chemical and Biochemical Perspectives*, S. Mann, J. Webb, R.J.P. Williams (eds.). VCH Publishers, Weinheim, 133-156, 1989.
24. Hay, D.I., et.al., "Phosphoprotein-inhibitors of calcium phosphate precipitation from salivary secretions," *Inorganic Perspectives in Biology and Medicine* 2, 271-285, 1979.
25. Juriense, A.C., et.al., "The absorption of acidic and basic homopolypeptides to whole bovine dental enamel," *Journal of Colloid and Interface Science*, 76, 212-219, 1980.
26. Sikes, C.S. and A.P. Wheeler, "A systematic approach to some questions of carbonate calcification," *Biomineralization and Biological Metal Accumulation*, P. Westbrook and E.W. DeJong (eds.). Reidel Publishing, Dordrecht, 285-289, 1983.
27. Wilbur, K.M. and A.M. Bernhardt, "Effects of amino acids, magnesium, and molluscan extrapallial fluid on crystallization of calcium carbonate: in vitro experiments," *Biological Bulletin*, 166, 251-259, 1984.
28. Mueller, E.M. and C.S. Sikes, "Adsorption and crystal growth modifications by polyanionic peptides and various polycations," Submitted.
29. Bailey, S.W., ed., "Hydrous Phyllosilicates: Exclusive of micas," *Reviews in Mineralogy*, Mineralogical Society of America, Washington, D.C., 19, 725, 1988.
30. Dominguez, J.M., and Occelli, M.L. in *Synthesis of Microporous Materials, part II*, Occelli, M.L., and Robson, H., Eds.; Van Norstrand 1992 (in press).
31. Occelli, M.L., and Drake, B., *J. Catal.*, to be submitted (1992).
32. Hochella, M.F., et. al., "Atomic structure and morphology of the albite (010) surface: An atomic force microscope and electron diffraction study," *Amer. Mineral.*, 75, 723-730, 1990.

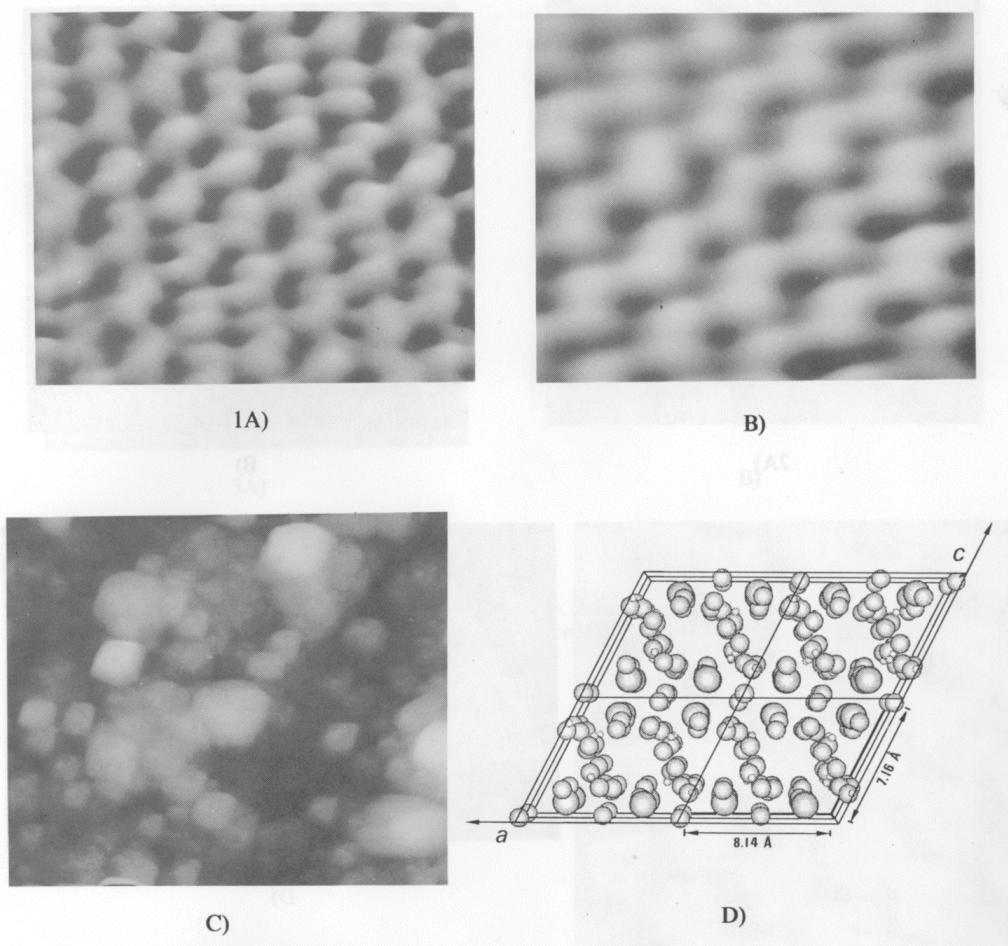
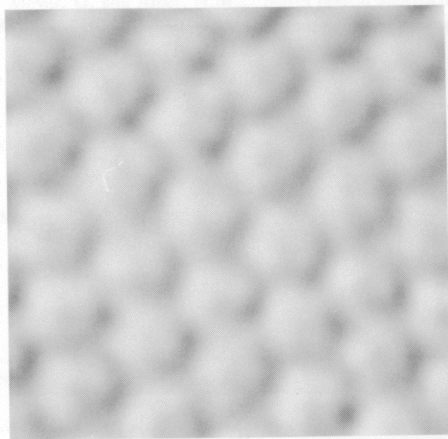
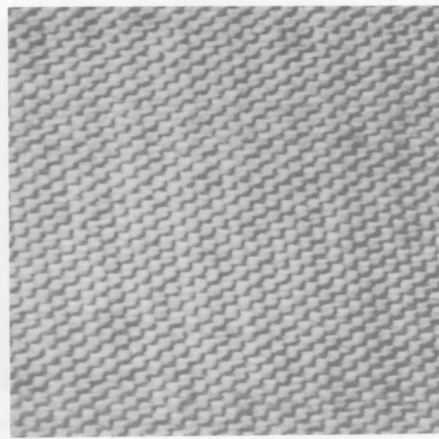


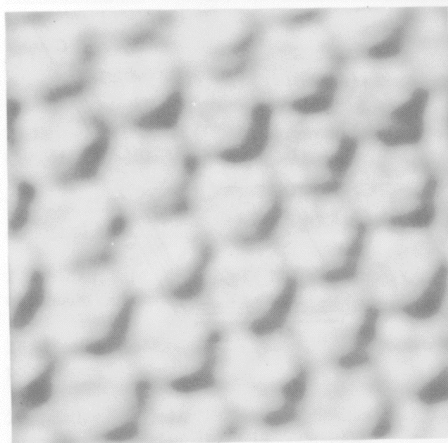
Fig. 1a) 3.0×3.0 nm image of the albite (010) surface. Note the six sided ring in the center of the image. (b) A 2.0×2.0 nm image using a second cantilever shows a similar sinuous structure to fig. 1a. (c) The 3.3×3.3 μm image shows the central square feature where fig. 1a was taken. (d) The four unit cell projection of the bulk structure is taken from a 5 \AA thick slice along the b axis⁶. Oxygen atoms predominate the six sided rings.



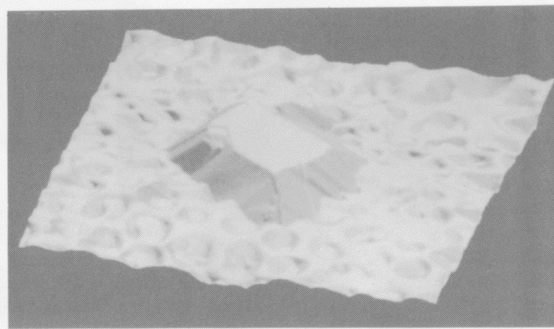
2A)



B)

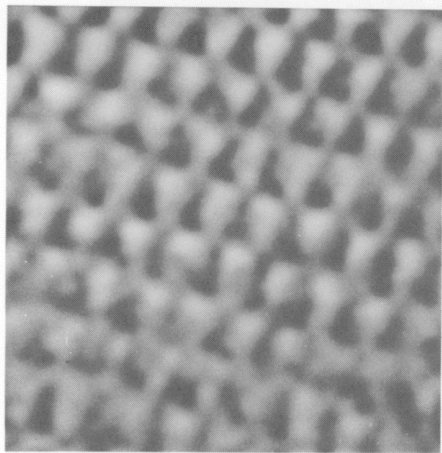


C)

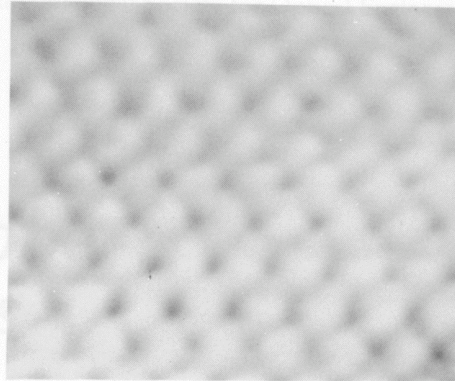


D)

Fig. 2a) The 2.7×2.7 nm image of the calcite basal plane shows a 5 \AA Ca-Ca atom hexagonal spacing. The image was taken from a single crystal grown onto a glass cover slip. (b) 16.0×16.0 nm image of what appears to be the carbonate (001) plane of calcite. (c) The 2.7×2.7 nm image was taken at the same location as fig. 2b. (d) $14.0 \times 14.0 \times 5.0 \text{ \mu m}$ image of a single calcite crystal attached to a glass cover slip using polyurethane.



3A)



B)

Fig. 3a) 7.0×7.0 nm image of the Mg-rectorite basal plane. A nearest neighbor distance of 9.1 ± 2.0 Å was measured. (b) 5.0×5.0 nm image of the basal plane of bentonite showed a 4.9 ± 0.5 Å hexagonal spacing.